

1 **Optical spectroscopic observations of gamma-ray blazars candidates I:**
2 **preliminary results**

3 A. Paggi¹, D. Milisavljevic¹, N. Masetti², E. Jiménez-Bailón³, V. Chavushyan⁴, R. D'Abrusco¹, F.
4 Massaro⁵,
5 M. Giroletti², Howard A. Smith¹, R. Margutti¹, G. Tosti⁶, J. R. Martinez Galarza¹, H.
6 Otí-Flóranes³, J. E. Grindlay¹

7 Received _____; accepted _____

version September 20, 2013: fm

¹Harvard - Smithsonian Astrophysical Observatory, 60 Garden Street, Cambridge, MA 02138,
USA

²INAF - Istituto di Astrofisica Spaziale e Fisica Cosmica di Bologna, via Gobetti 101, 40129,
Bologna, Italy

³Instituto de Astronomía, Universidad Nacional Autónoma de México, Apdo. Postal 877, En-
senada, 22800 Baja California, México

⁴Instituto Nacional de Astrofísica, Óptica y Electrónica, Apartado Postal 51-216, 72000 Puebla,
México

⁵SLAC - National Laboratory and Kavli Institute for Particle Astrophysics and Cosmology,
2575 Sand Hill Road, Menlo Park, CA 94025, USA

⁶Dipartimento di Fisica, Università degli Studi di Perugia, 06123 Perugia, Italy

Submitted to Astronomical Journal.

8 **ABSTRACT**

9 A significant fraction ($\sim 30\%$) of the gamma-ray sources listed in the second *Fermi*
LAT (2FGL) catalog are still of unknown origin, being not yet associated with counter-
parts at lower energies. Using the available information at lower energies and optical
spectroscopy on the selected counterparts of these gamma-ray objects we can pinpoint
their exact nature. Here we report optical spectroscopic observations of a sample of
5 gamma-ray blazar candidates selected on the basis of their infrared WISE colors
or of their low-frequency radio properties. Blazars come in two main classes: BZBs
and BZQs, with the latter similar to the former except for the stronger optical emis-
sion lines. For three of our sources the almost featureless optical spectra obtained
confirm their BZB nature, while for the source WISEJ022051.24+250927.6 we ob-
serve emission lines with equivalent width $EW \sim 31 \text{ \AA}$, identifying it as a BZQ with
 $z = 0.48$. The source WISEJ064459.38+603131.7, although not featuring a clear radio
counterpart, shows a blazar-like spectrum with weak emission lines with $EW \sim 7 \text{ \AA}$,
yielding a redshift estimate of $z = 0.36$. In addition we report optical spectroscopic
observations of 4 WISE sources associated with known gamma-ray blazars without a
firm classification or redshift estimate. For all of these latter sources we confirm their
BZB, with a tentative redshift estimate for the source WISEJ100800.81+062121.2 of
 $z = 0.65$.

10 *Subject headings:* galaxies: active - galaxies: BL Lacertae objects - radiation mechanisms:
11 non-thermal

1. Introduction

12
13 About 1/3 of the γ -ray sources listed in the 2nd *Fermi* catalog (2FGL, [Nolan et al. 2012](#)) have
14 not yet been associated with counterparts at lower energies. A precise knowledge of the number
15 of unidentified gamma-ray sources (UGSs) is extremely relevant since for example it could help
16 to provide the tightest constraint on the dark matter models ever determined ([Abdo et al. 2013](#)).
17 Many UGSs could be blazars, the largest identified population of extragalactic γ -ray sources, but
18 how many are actually blazars is not yet known due in part to the incompleteness of the catalogs
19 used for the associations ([Ackermann et al. 2011](#)). The first step to reduce the number of UGSs is
20 therefore to recognize those that could be blazars.

21 Blazars are the rarest class of Active Galactic Nuclei, dominated by non-thermal radiation
22 over the entire electromagnetic spectrum (e.g., [Urry & Padovani 1995](#); [Giommi, Padovani, &](#)
23 [Polenta 2013](#)). Their observational properties are generally interpreted in terms of a relativistic
24 jet aligned within a small angle to our line of sight ([Blandford & Rees 1978](#)). According to the
25 nomenclature proposed by [Massaro et al. \(2011a\)](#), Blazars have been classified as: BZBs and
26 BZQs, with the latter similar to the former except for the stronger optical emission lines and
27 the higher radio polarization. In particular, if the only spectral features observed are emission
28 lines with rest frame equivalent width $EW \leq 5 \text{ \AA}$ the object is classified as a BZB ([Stickel et al.](#)
29 [1991](#); [Stoeckl & Reuter 1997](#)), otherwise it is classified as BZQ ([Laurent-Muehleisen et al. 1999](#);
30 [Massaro et al. 2011a](#)).

31 The blazar spectral energy distributions (SEDs) typically show two peaks: one in the range
32 of radio - soft X-rays, due to synchrotron emission by highly relativistic electrons within the jet;
33 and another one at hard X-ray or γ -ray energies, interpreted as inverse Compton upscattering by
34 the same electrons of the seed photons provided by the synchrotron emission ([Inoue & Takahara](#)
35 [1996](#)) with the possible addition of seed photons from outside the jets yielding contributions to
36 the non-thermal radiations due to external inverse Compton scattering (see [Dermer & Schlickeiser](#)

37 1993; Dermer et al. 2009) often dominating their γ -ray outputs (Aharonian et al. 2009; Ackermann
38 et al. 2011).

39 Recently, D’Abrusco et al. (2013) proposed an association procedure to recognize γ -ray
40 blazar candidates on the basis of their positions in the three-dimensional WISE color space. As a
41 matter of fact, blazars - whose emission is dominated by beamed, non thermal emission - occupy
42 a defined region in such a space, well separated from that occupied by other sources in which
43 thermal emission prevails (Massaro et al. 2011b; D’Abrusco et al. 2012). Applying this method,
44 Cowperthwaite et al. (2013) recently identified thirteen gamma-ray emitting blazar candidates
45 from a sample of 102 previously unidentified sources selected from Astronomer’s Telegrams and
46 the literature.

47 Massaro et al. (2013a) applied the classification method proposed by D’Abrusco et al. (2013)
48 to the 258 UGSs and 210 active galaxies of uncertain type (AGUs) listed in the 2FGL (Nolan
49 et al. 2012) finding candidate blazar counterparts for 141 of the UGSs and 125 of the AGUs.
50 The classification method proposed by D’Abrusco et al. (2013), however, can only be applied to
51 sources detected in all 4 WISE bands, i.e., 3.4, 4.6, 12 and 22 μm .

52 Using the X-ray emission in place of the 22 μm detection, Paggi et al. (2013) proposed a
53 method to select γ -ray blazar candidates among *Swift*-XRT sources considering those that feature
54 a WISE counterpart detected at least in the first 3 bands, and with IR colors compatible with
55 the 90% two-dimensional densities of known γ -ray blazar evaluated using the Kernel Density
56 Estimation (KDE) technique (see, e.g., D’Abrusco, Longo, & Walton 2009; Laurino et al. 2011;
57 Richards et al. 2004, and reference therein), so selecting 37 new γ -ray blazar candidates. Similarly,
58 using the radio emission as additional information, Massaro et al. (2013c) investigated all the
59 radio sources in NVSS and SUMSS surveys that lie within positional uncertainty region of *Fermi*
60 UGSs and, considering those sources with IR colors compatible with the 90% two-dimensional
61 KDE densities of known γ -ray blazar, selected 66 additional γ -ray blazar candidates.

Table 1: WISE sources discussed in this paper. In the upper part of the Table we list the γ -ray blazar candidates associated with UGSs or AGUs, while in the lower part we list the sources associated with known γ -ray blazars. Column description is given in the main text (see Sect. 3).

WISE NAME	RA J2000	DEC J2000	OTHER NAME	NAME 2FGL	NOTES
J022051.24+250927.6	02:20:51.24	+25:09:27.6	NVSSJ022051+250926	2FGLJ0221.2+2516	UGS X-KDE
J050558.78+611335.9	05:05:58.79	+61:13:35.9	NVSSJ050558+611336	2FGLJ0505.9+6116	AGU WISE
J060102.86+383829.2	06:01:02.87	+38:38:29.2	WN0557.5+3838	2FGLJ0600.9+3839	UGS WENSS
J064459.38+603131.7	06:44:59.39	+60:31:31.8		2FGLJ0644.6+6034	UGS WISE
J104939.34+154837.8	10:49:39.35	+15:48:37.9	GB6J1049+1548	2FGLJ1049.4+1551	AGU R-KDE
J022239.60+430207.8	02:22:39.61	+43:02:07.9	BZBJ0222+4302	2FGLJ0222.6+4302	A, Z=0.444?
J100800.81+062121.2	10:08:00.82	+06:21:21.3	BZBJ1008+0621	2FGLJ1007.7+0621	B, CAND
J131443.81+234826.7	13:14:43.81	+23:48:26.8	BZBJ1314+2348	2FGLJ1314.6+2348	B, CAND
J172535.02+585140.0	17:25:35.03	+58:51:40.1	BZBJ1725+5851	2FGLJ1725.2+5853	B, CAND

62 Finally, [Massaro et al. \(2013b\)](#) investigated the low-frequency radio emission of blazars and
63 searched for sources with similar features combining the information derived from the WENSS
64 and NVSS surveys, identifying 26 γ -ray candidate blazars in the *Fermi* LAT the positional
65 uncertainty region of 21 UGSs.

66 In this paper we report on optical spectra acquired using MMT, Loiano and OAN telescopes
67 of 5 WISE γ -ray blazar candidates - counterparts of three UGSs and one AGU - selected with the
68 three methods described before (position in the three dimensional WISE IR colors space, X-ray
69 detection plus position in the two dimensional WISE IR color space and low-frequency radio
70 properties), in order to identify their nature and to test the reliability of these different approaches
71 in selecting γ -ray candidate blazars. In addition, we also present optical spectra of 4 known γ -ray
72 blazars with uncertain redshift estimates or unknown classification (BZB vs BZQ,) ([Ackermann](#)
73 [et al. 2011](#); [Nolan et al. 2012](#)) with a WISE counterpart identified by [D’Abrusco et al. \(2013\)](#).

74 The paper is structured as follows: in Sect. 2 we describe the observation procedures and the
75 data reduction process adopted, in Sect. 3 we present our results on individual sources and discuss
76 them in Sect. 4, while in Sect. 5 we present our conclusions.

77 Throughout this paper USNO-B magnitudes are reported as photographic magnitudes, SDSS
78 magnitudes are reported in AB system, and 2MASS magnitudes are reported in VEGA system.

79 2. Observations

80 The spectroscopic observations for all sources with the exception of WISEJ022239.60+430207.8
81 and WISEJ104939.34+154837.8 were carried out during nights of January 17 and 18, 2013 with
82 the 6.5 m Multiple Mirror Telescope (MMT) and its Blue Channel Spectrograph with a 300 gpm
83 grating and a 2x180” slit, for a resolution of about 6.2 Å. The spectra covered about 4800 Å,
84 centered on 5900 Å, and the 3072 x 1024 pixel ccd22 was used as a detector. For each target,

85 we obtained a series of two spectra, with exposure times of 1800-2700 s and combined them
86 during the reduction process. We used helium-neon-argon calibration lamps before and after each
87 exposure. A few spectroscopic standards were also observed and used to remove the spectral
88 response and to fluxcalibrate the data.

89 The object WISEJ022239.60+430207.8 was observed spectroscopically with the 1.5-meter
90 “G.D. Cassini” telescope in Loiano (Italy) equipped with the BFOSC spectrograph, which carries
91 a 1300×1340 pixels EEV CCD. Two 1800-s spectroscopic frames were secured on 3 December
92 2012, with start times at 21:12 and 21:44 UT, respectively. Data were acquired using Grism #4
93 and with a slit width of 2'0, giving a nominal spectral coverage between 3500 and 8700 Å and a
94 dispersion of 4.0 Å/pix. Wavelength calibration was obtained with Helium-Argon lamps.

95 Likewise, three optical spectra of 1800 s each of source WISEJ104939.34+154837.8 were
96 secured with the 2.1-meter telescope of the Observatorio Astronómico Nacional (OAN) in San
97 Pedro Mártir (México) on 2 May 2013 with mid-exposure time 04:58 UT. The telescope carries
98 a Boller & Chivens spectrograph and a 1024x1024 pixels E2V-4240 CCD. A slit width 2''.5 was
99 used. The spectrograph was tuned in the $\sim 4000 \div 8000$ Å range (grating 300 l/mm), with a
100 resolution of 4 Å/pixel, which corresponds to 8 Å (FWHM).

101 The telescope carries a Boller & Chivens spectrograph and a 300×1024 pixels E2V-4240
102 CCD. The spectrograph was tuned in the 4000÷8000 Å range (grating 300 l/mm), with a
103 resolution of 4 Å per pixel, which corresponds to 8 Å (FWHM), and a 2''.5 slit. This yielded a
104 3300÷7700 spectral coverage and a 4.5 Å/pix dispersion. Data were wavelength calibrated using
105 Copper-Helium-Neon-Argon lamps, while for flux calibration spectrophotometric standard stars
106 were observed twice during every night of the observing run.

107 The data reduction was carried out using the IRAF package of NOAO including bias
108 subtraction, spectroscopic flat fielding, optimal extraction of the spectra and interpolation of the
109 wavelength solution. All spectra were reduced and calibrated employing standard techniques in

110 IRAF and our own IDL routines (see, e.g., [Matheson et al. 2008](#)).

111 **3. Results on individual sources**

112 In Table 1 we list the WISE sources presented in this paper. In the upper part of the table
113 we report the γ -ray blazar candidates associated with UGSs or AGUs; in particular, in the NAME
114 2FGL column we indicate the name of associated *Fermi* source, in the OTHER NAME column
115 we indicate the relative radio counterpart and in the NOTES column we indicate with X-KDE,
116 WISE, WENSS and R-KDE the source selected as γ -ray blazar candidate according to [Paggi et](#)
117 [al. \(2013\)](#), [Massaro et al. \(2013a\)](#), [Massaro et al. \(2013b\)](#) and [Massaro et al. \(2013c\)](#), respectively.
118 In the lower part of the Table we list the sources associated with known γ -ray blazars with the
119 classification method proposed by [D’Abrusco et al. \(2013\)](#), with additional information from
120 BZCAT catalog ([Massaro et al. 2011a](#)); in particular, for these sources in the OTHER NAME
121 column we indicate the associated blazar name, and in the NOTES column we report the class
122 depending on the probability of the WISE source to be compatible with the model of the WISE
123 *Fermi* Blazar locus ([D’Abrusco et al. 2013](#), see Sect. 4) and we indicate with CAND the sources
124 listed as blazar candidates or the reported redshift estimate (see [Massaro et al. 2011b](#)).

125 Optical images of the fields containing these sources are presented in Fig. 1, while the
126 extracted spectra are presented in Figs. 2 and 3. The discussion for each individual target is given
127 in the following sub-sections, and the main observational results are presented in Table 2.

128 **3.1. WISEJ022051.24+250927.6**

129 This source lies in the positional uncertainty region at 95% level of confidence of the *Fermi*
130 UGS 2FGLJ0221.2+2516 as reported in the 2FGL catalog ([Nolan et al. 2012](#)), and it is associated
131 with the NVSS ([Condon et al. 1998](#)) radio source NVSSJ022051+250926 with a $\sim 1''$ angular

132 separation. The USNO-B (Monet et al. 2003) optical counterpart, at $\sim 0.1''$, features magnitudes
 133 B1=18.74 mag, R1=18.82 mag, B2=19.80 mag, R2=19.51 mag and I2=18.10 mag. Paggi et al.
 134 (2013) showed that this source is positionally consistent ($\sim 4.7''$) with the X-ray *Swift* source
 135 SWXRTJ022051.5+250930, featuring an unabsorbed flux $\sim 1.3 \times 10^{-13}$ erg cm $^{-2}$ s $^{-1}$. On the
 136 basis of its position in the two dimensional WISE IR color space - that is the [3.4]-[4.6] [4.6]-[12]
 137 color plane - this source has been selected by the same authors as γ -ray blazar candidate. The
 138 spectrum of WISEJ022051.24+250927.6 presented in Fig. 2a clearly shows strong emission lines
 139 that we identify as broad Mg II ($EW = 30.8 \pm 0.7 \text{ \AA}$), narrow [Ne v] ($EW = 1.8 \pm 0.3 \text{ \AA}$), narrow
 140 [O II] ($EW = 1.7 \pm 0.3 \text{ \AA}$), narrow [Ne III] ($EW = 1.1 \pm 0.4 \text{ \AA}$) and narrow [O III] ($EW = 15.8 \pm 0.3$
 141 \AA), yielding a redshift $z = 0.4818 \pm 0.0002$.

142 3.2. WISEJ050558.78+611335.9

143 This source is the candidate counterpart of the *Fermi* AGU 2FGLJ0505.9+6116 proposed
 144 by Massaro et al. (2013a), lying within the LAT positional uncertainty region at 95% level of
 145 confidence. It is associated with the radio sources NVSSJ050558+611336 ($\sim 0.5''$) and WENSS
 146 (Rengelink et al. 1997) WN0501.4+6109 ($\sim 2.3''$). The closest source in the USNO-B catalog, at
 147 $\sim 0.4''$, features magnitudes R1=18.71 mag, B2=20.73 mag, R2=18.67 mag and I2=17.30 mag,
 148 while the closest counterpart in the SDSS (Pâris et al. 2012) survey is SDSSJ050558.77+611336.1
 149 with magnitudes u=21.66 mag, g=20.58 mag, r=19.65 mag, i=19.02 mag and z=18.58 mag.
 150 The optical source J0505+6113 ($\sim 0.4''$) has been observed with Marcario Low Resolution
 151 Spectrograph on the Hobby-Eberly Telescope (Shaw et al. 2013) without yielding a redshift
 152 estimate. WISEJ050558.78+611335.9 is also associated with the near 2MASS (Skrutskie et al.
 153 2006) IR counterpart 2MASSJ05055874+6113359 ($\sim 0.1''$) with magnitudes H=16.228 mag
 154 and K=15.156 mag, with a lower limit on the J magnitude of 17.136 mag. According to the
 155 source position in the three dimensional WISE IR color space, this source has been selected by

156 [Massaro et al. \(2013a\)](#) as γ -ray BZB candidate. As shown in Figure 2b the featureless spectrum
157 of WISEJ050558.78+611335.9 confirms this classification of the WISE source.

158 **3.3. WISEJ060102.86+383829.2**

159 The Fermi UGS 2FGLJ0600.9+3839 has been associated with the gamma-ray blazar
160 candidate WISEJ060102.86+383829.2 by [Massaro et al. \(2013a\)](#). The correspondent optical
161 counterpart in the USNO-B catalog, at $\sim 0.1''$, features magnitudes R1=19.11 mag, R2=19.84 mag
162 and I2=18.48 mag. According to [Paggi et al. \(2013\)](#) this source is positionally consistent ($\sim 0.6''$)
163 with the X-ray *Swift* source SWXRTJ060102.8+383829 having a 0.3 – 10 keV unabsorbed flux
164 $\sim 2.3 \times 10^{-13}$ erg cm $^{-2}$ s $^{-1}$. It is also associated with the radio sources NVSSJ060102+383828
165 ($\sim 0.5''$) and WN0557.5+3838 ($\sim 0.8''$); in particular, based on the source low-frequency radio
166 properties, [Massaro et al. \(2013b\)](#) classified this source as a γ -ray blazar candidate. As shown in
167 Figure 2c the featureless spectrum of WISEJ050558.78+611335.9 confirms its BZB nature.

168 **3.4. WISEJ064459.38+603131.7**

169 This source is the gamma-ray blazar candidate counterpart of the UGS 2FGLJ0644.6+6034
170 proposed by [Massaro et al. \(2013a\)](#). The USNO-B optical counterpart lying at $\sim 0.4''$ features
171 magnitudes B1=19.44 mag, R1=19.03 mag, B2=19.33 mag, R2=18.23 mag and I2=18.28 mag,
172 while the IR counterpart 2MASSJ06445937+6031318 ($\sim 0.1''$) features magnitudes J=16.923
173 mag, H=15.979 mag and K=15.371 mag. According to [Paggi et al. \(2013\)](#) this source is
174 positionally consistent ($\sim 0.1''$) with the X-ray *Swift* source SWXRTJ064459.9+603132 with
175 a 0.3 – 10 keV unabsorbed flux $\sim 2.1 \times 10^{-13}$ erg cm $^{-2}$ s $^{-1}$. This source does not feature any
176 obvious radio counterpart; nevertheless, basing on its position in the three dimensional WISE IR
177 color space, this source has been selected by [Massaro et al. \(2013a\)](#) as γ -ray blazar candidate.

178 The spectrum of WISEJ064459.38+603131.7 presented in Figure 2d show an almost featureless
179 continuum with narrow Mg II ($EW = 6.1 \pm 0.4 \text{ \AA}$), and weak detections of narrow H β ($EW = 4 \pm 2$
180 \AA) and narrow H δ ($EW = 7 \pm 2 \text{ \AA}$) emission lines (the latter probably affected by contamination
181 from noise/cosmic rays), reminiscent of weak emission line quasar spectra (see e.g., [Shemmer et](#)
182 [al. 2006, 2009](#), and references therein), and yielding $z = 0.3582 \pm 0.0008$.

183 **3.5. J104939.34+154837.8**

184 This source lies in the positional uncertainty region of the *Fermi* AGU 2FGLJ1049.4+1551.
185 It is associated with the radio sources NVSSJ104939+154838 ($\sim 1.0''$) and FIRST ([Becker,](#)
186 [White, & Helfand 1995](#)) FIRSTJ104939.3+154837 ($\sim 0.3''$), and with the optical counterpart
187 SDSSJ104939.35+154837.6, with magnitudes u=18.58 mag, g=18.11 mag, r=17.64 mag, i=17.36
188 mag and z=17.13 mag. Furthermore this source is associated 2MASSJ10493935+1548374
189 ($\sim 0.4''$) with magnitudes H=14.899 mag and K=14.144 mag and J=15.622 mag.

190 Applying the same selection method presented by [Massaro et al. \(2013c\)](#), the radio emission
191 from this source and its position in the two dimensional WISE IR color space classify this source
192 as a γ -ray blazar candidate. The spectrum of WISEJ104939.34+154837.8 presented in Figure 2e
193 shows an almost featureless spectrum typical of BZBs, with two weak absorption lines consistent
194 with Ca II H & K ($EW = 0.70 \pm 0.13 \text{ \AA}$ and $EW = 0.60 \pm 0.10 \text{ \AA}$, respectively) located at observed
195 wavelength of 5220.6 and 5266.7 \AA . Given this identification, the estimated redshift for this
196 source is $z = 0.3271 \pm 0.0003$.

197 **3.6. WISEJ022239.60+430207.8**

198 [D'Abrusco et al. \(2013\)](#) found that WISEJ022239.60+430207.8 is the IR counterpart
199 of 2FGLJ0222.6+4302, associated in the 2FGL and in the 2LAC catalogs ([Ackermann et](#)

200 al. 2011; Nolan et al. 2012) with the blazar BZBJ0222+4302, also known as 3C66A. This
201 is a well known TeV detected BZB with a long and debated redshift estimate history. In
202 fact a past tentative measurement of $z = 0.444$ (Miller, French, & Hawley 1978; Kinney
203 et al. 1991) is based on the measurement of single, weak line (the optical spectrum is not
204 published, see Landt & Bignall 2008). There have also been suggestions that 3C66A is a
205 member of a cluster at $z \sim 0.37$ (Butcher et al. 1976; Wurtz et al. 1993, 1997), while a lower
206 limit of $z > 0.096$ based on the expected equivalent widths of absorption features in the
207 blazar host galaxy has been set by Finke et al. (2008), and an upper limit of $z < 0.58$ has
208 been set by Yang & Wang (2010) comparing the measured and intrinsic VHE spectra due to
209 extragalactic background light absorption. In the same way, an estimate for the blazar redshift
210 of $z = 0.34 \pm 0.05$ was found by Prandini et al. (2010). Recently, Furniss et al. (2013) making
211 use of far-ultraviolet HST/COS spectra, evaluated for 3C66A a redshift range $0.3347 < z < 0.41$
212 at 99% confidence. The source WISEJ022239.60+430207.8 is also associated with the radio
213 source NVSSJ022239+430208 $\sim 1.5''$, while the closest source in the USNO-B catalog, at
214 $\sim 0.1''$, has brightnesses of B1=15.88.44 mag, R1=15.15 mag, B2=14.94 mag, R2=14.35 mag
215 and I2=12.59 mag. The optical source J0222+4302 ($\sim 1.4''$) has been observed with the Low
216 Resolution Imaging Spectrograph at the W. M. Keck Observatory (Shaw et al. 2013) without
217 yielding a redshift estimate. On the other hand, the IR counterpart 2MASSJ02223961+4302078
218 ($\sim 0.1''$) features magnitudes J=12.635 mag, H=11.880 mag and K=11.151 mag. The spectrum
219 of WISEJ022239.60+430207.8 presented in Figure 3a shows a featureless spectrum typical of
220 BZBs so, even if we are not able to obtain a spectroscopic redshift estimate, we confirm the blazar
221 nature of WISEJ022239.60+430207.8.

3.7. WISEJ100800.81+062121.2

222
223 D'Abrusco et al. (2013) selected this WISE source as the IR counterpart of blazar candidate

224 BZBJ1008+0621, associated with the gamma-ray source 2FGLJ1007.7+0621 (Ackermann
225 et al. 2011; Nolan et al. 2012). This WISE source is also associated with the radio sources
226 NVSSJ100800+062121 ($\sim 0.6''$) and FIRSTJ100800.8+062121 ($\sim 0.3''$). It is also associated
227 with a USNO-B source ($\sim 0.2''$) with brightnesses of B1=17.72 mag, R1=16.72 mag, B2=18.54
228 mag, R2=16.73 mag and I2=16.74 mag, and with the SDSS source SDSSJ100800.81+062121.2
229 ($\sim 0.1''$) with magnitudes u=18.63 mag, g=18.11 mag, r=17.64 mag, i=17.28 mag and z=17.02
230 mag. The optical source J1008+0621 ($\sim 0.5''$) has been observed with the Low Resolution
231 Imaging Spectrograph at the W. M. Keck Observatory (Shaw et al. 2013) without yielding a
232 redshift estimate. On the other hand, its near IR counterpart 2MASSJ10080081+0621212 ($\sim 0.1''$)
233 has magnitudes J=14.121 mag, H=13.345 mag and K=12.458 mag, and has been studied by
234 Urrutia et al. (2009) with optical spectroscopy that yielded a blazar classification with $z = 1.72$.
235 The spectrum of WISEJ100800.81+062121.2 presented in Figure 3b shows an almost featureless
236 spectrum with only a weak narrow absorption line that we tentatively identify as Mg II, yielding a
237 redshift estimate of $z = 0.6495$.

238 3.8. WISEJ131443.81+234826.7

239 This WISE source has been selected by D'Abrusco et al. (2013) as the IR counterpart of *Fermi*
240 source 2FGLJ1314.6+2348, associated with the blazar candidate BZBJ1314+2348 (Ackermann
241 et al. 2011; Nolan et al. 2012). This WISE source is also associated with the radio sources
242 NVSSJ131443+234827 ($\sim 0.2''$) and FIRSTJ131443.8+234826 ($\sim 0.1''$) (Bourda et al. 2011;
243 Petrov 2011; Linford et al. 2011, 2012). The associated IR source 2MASSJ13144382+2348267
244 ($\sim 0.1''$) has brightnesses J=15.514 mag, H=14.688 mag and K=13.832 mag (Mao 2011). Its
245 optical counterpart found in the USNO-B catalog ($\sim 0.1''$) features magnitudes B1=17.05,
246 R1=15.43 mag, B2=17.80 mag, R2=17.06 mag and I2=16.15 mag, while the closest SDSS source
247 is SDSSJ131443.80+234826.7 ($\sim 0.1''$) with magnitudes u=17.55 mag, g=17.13 mag, r=16.80

248 mag, $i=16.54$ mag and $z=16.31$ mag. The optical source J1725+5851 ($\sim 1''$) has been observed
249 with the Low Resolution Imaging Spectrograph at the W. M. Keck Observatory (Shaw et al. 2013)
250 without yielding a redshift estimate. The spectrum of WISEJ131443.81+234826.7 presented in
251 Figure 3c shows a featureless spectrum typical of BZBs.

252 3.9. WISEJ172535.02+585140.0

253 D’Abrusco et al. (2013) found this WISE source to be the counterpart of the *Fermi* source
254 2FGLJ1725.2+5853, associated in the 2FGL and 2LAC catalogs (Ackermann et al. 2011; Nolan et
255 al. 2012) with the BZB candidate BZBJ1725+5851 (Massaro et al. 2011a). This WISE source is
256 also associated with the radio sources NVSSJ172535+585139 ($\sim 0.8''$), FIRSTJ172535.0+585139
257 ($\sim 0.3''$) and WN1724.8+5854 ($\sim 2.2''$). The closest USNO-B source ($\sim 0.3''$) has brightnesses
258 of $B_1=17.56$ mag, $R_1=16.54$ mag, $B_2=17.14$ mag, $R_2=16.15$ mag and $I_2=15.47$ mag, while
259 the closest SDSS source is SDSSJ172535.01+585139.9 ($\sim 0.2''$) with magnitudes $u=18.36$
260 mag, $g=17.90$ mag, $r=17.55$ mag, $i=17.27$ mag and $z=17.00$ mag. The associated IR source
261 2MASSJ17253500+5851400 ($\sim 0.1''$) has brightnesses $J=15.549$ mag, $H=14.705$ mag and
262 $K=13.952$ mag.

263 Our optical spectrum of WISEJ172535.02+585140.0, with its $2''$ slit, is presented in
264 Figure 3d; it shows a featureless spectrum typical of BZBs. This supports our identification
265 of WISEJ172535.02+585140.0 as the likely counterpart of BZBJ1725+5851. The other
266 optical-IR sources nearby to the WISE position are SDSSJ172535.03+585140.0 ($\sim 0.1''$) and
267 SSTXFLSJ172535.0+585139 ($\sim 0.1''$). (Richards et al. 2004) and (Marleau et al. 2007), report
268 that these source are counterparts of 2MASSJ17253500+5851400, but while the former authors
269 indicate for this source a photometric redshift estimate of $z = 2.025$ with a 53.3% probability of
270 the source redshift lying in the range $2.00 < z < 2.20$, the latter authors report a tentative redshift
271 upper limit $z < 0.2974$ estimated from the 4000 \AA break. While the latter estimate is compatible

272 with our evidence of this source being a BZB (redshift of BZB in BZCAT range from 0.023 to
273 1.34, peaking at $z \sim 0.3$), the former is unlikely for such a source, indicating either a doubtful
274 association of SDSSJ172535.03+585140.0 with 2MASSJ17253500+5851400 (or of the 2MASS
275 source with WISEJ172535.02+585140.0) or an unreliable photometric redshift estimate.

276 4. Discussion

277 The optical spectra we obtained with MMT, Loiano and OAN telescopes provide the first
278 confirmation of the association procedure and the tentative classification of gamma-ray blazar
279 candidates developed by [D’Abrusco et al. \(2013\)](#) and adopted by [Massaro et al. \(2013a\)](#), as well
280 as those proposed in [Massaro et al. \(2013b\)](#), [Paggi et al. \(2013\)](#) and [Massaro et al. \(2013c\)](#).

281 The four WISE sources associated with known γ -ray blazar counterparts have been
282 tentatively classified as BZBs by [D’Abrusco et al. \(2013\)](#). In fact, the authors assign to every
283 source a class A, B, or C depending on the probability of the WISE source to be compatible with
284 the model of the WISE *Fermi* Blazar locus (WFB) in the three dimensional color space: class A
285 sources are considered the most reliable candidate blazars for the high-energy source, while class
286 B and class C sources are less compatible with the WFB locus but are still deemed as gamma-ray
287 blazar candidates. According to this classification, the source WISEJ022239.60+430207.8 is a
288 class A BZB γ -ray candidate, while the other sources here analyzed are class B BZBs. The spectra
289 presented in [Figure 3](#) confirm for all these sources their BZB nature. In addition, for the source
290 WISEJ100800.81+062121.2 (associated with the blazar BZBJ1008+0621) we provide for the first
291 time a tentative redshift estimate $z = 0.65$.

292 In addition, optical spectroscopy can be used to test the predictions of the different association
293 procedure that are used to find γ -ray blazar candidates lying in the uncertainty regions at 95%
294 level of confidence as reported in the 2FGL catalog ([Nolan et al. 2012](#)) of UGSs or AGUs listed in

295 the 2FGL. In particular the sources WISEJ050558.78+611335.9 and WISEJ064459.38+603131.7
296 are selected by [Massaro et al. \(2013a\)](#) as class C γ -ray blazar candidates of BZB and undefined
297 type, respectively; WISEJ060102.86+383829.2 is selected as γ -ray blazar candidate by [Massaro](#)
298 [et al. \(2013b\)](#) on the basis of its low-frequency radio properties; WISEJ022051.24+250927.6 is
299 selected as γ -ray blazar candidate by [Paggi et al. \(2013\)](#) combining its *Swift* X-ray emission and
300 its IR WISE colors; finally, WISEJ104939.34+154837.8 is selected as γ -ray blazar candidate by
301 [Massaro et al. \(2013c\)](#) combining its radio emission and its IR WISE colors. As shown in Figure
302 2 all these WISE sources show a blazar-like optical spectrum.

303 In particular, WISEJ050558.78+611335.9 and WISEJ060102.86+383829.2 show featureless
304 BZB spectra, while WISEJ104939.34+154837.8 shows an almost featureless spectrum with weak
305 absorption lines consistent with Ca II H & K yielding a redshift estimate $z = 0.33$; the EW of these
306 line - 0.7 \AA - is however consistent with the BZB definition given in Sect. 1.

307 On the other hand WISEJ022051.24+250927.6 and WISEJ064459.38+603131.7 show BZQ
308 type spectra with emission lines with $EW \sim 30 \text{ \AA}$ and $EW \sim 6 \text{ \AA}$, yielding redshift values of
309 $z = 0.48$ and $z = 0.36$, respectively. The spectrum of WISEJ064459.38+603131.7, in particular, is
310 somewhat reminiscent of weak emission line quasar spectra ([Shemmer et al. 2006, 2009](#)), but the
311 blazar identification for this source appears problematic: in fact, the absence of radio emission is
312 puzzling since blazars, by definition, are radio loud sources and radio-quiet blazars are extremely
313 rare objects ([Londish et al. 2004](#)).

314 The blazar nature of our candidates is also reinforced when comparing their multi-
315 wavelength SEDs with those of the known γ -ray blazars, presented in Figures 4 and 5 in Appendix
316 A, respectively. Despite the non simultaneity of the observations, we can clearly see the two main
317 spectral components - that is, lower energy synchrotron and higher energy inverse Compton -
318 typical of blazar SEDs.

319

5. Conclusions

320 We presented optical spectroscopic observations for a sample of five γ -ray blazar candidates
321 selected with different methods based on their radio to IR properties, and for a sample of four
322 WISE counterparts to known γ -ray blazar.

323 The main results of our analysis are summarized as follows:

- 324 1. We confirm the blazar nature of all the sources associated with known γ -ray blazar. In
325 addition, we obtain for the first time a tentative redshift estimate $z = 0.65$ for the blazar
326 BZBJ1008+0621.
- 327 2. We confirm the blazar nature of all the γ -ray blazar candidates selected by [Massaro et](#)
328 [al. \(2013a\)](#), [Massaro et al. \(2013b\)](#), [Paggi et al. \(2013\)](#) and [Massaro et al. \(2013c\)](#). In
329 addition, we obtain for WISEJ104939.34+154837.8, WISEJ022051.24+250927.6 and
330 WISEJ064459.38+603131.7 redshift estimates of $z = 0.33$, $z = 0.48$ and $z = 0.36$,
331 respectively.
- 332 3. The source WISEJ064459.38+603131.7, in particular, is intriguing since it shows an almost
333 featureless continuum with weak emission lines reminiscent of weak emission line quasar
334 spectra ([Shemmer et al. 2006, 2009](#)), but it lacks any obvious radio counterpart, which is
335 required for a blazar classification ([Giommi et al. 2012](#); [Giommi, Padovani, & Polenta](#)
336 [2013](#)).

337 While these preliminary results seem to confirm the effectiveness of the classification method
338 presented by [D’Abrusco et al. \(2013\)](#) and of the selection methods presented by [Massaro et](#)
339 [al. \(2013a\)](#), [Massaro et al. \(2013b\)](#), [Paggi et al. \(2013\)](#) and [Massaro et al. \(2013c\)](#), additional
340 ground-based, optical and near IR, spectroscopic follow up observations of a larger sample of
341 γ -ray blazar candidates are needed to confirm the nature of the selected sources and to obtain

342 their redshift. This will yield to a direct confirmation of the reliability of the association methods
343 proposed by [Massaro et al. \(2013a\)](#), [Massaro et al. \(2013b\)](#) and [Paggi et al. \(2013\)](#).

344

345

346 We are grateful to E. Falco for his valuable support and for the enjoyable nightly discussions
347 at MMT telescope. This work is supported by the NASA grants NNX12AO97G. The work at SAO
348 is partially supported by the NASA grant NNX13AP20G. R. D’Abrusco gratefully acknowledges
349 the financial support of the US Virtual Astronomical Observatory, which is sponsored by the
350 National Science Foundation and the National Aeronautics and Space Administration. The work
351 by G. Tosti is supported by the ASI/INAF contract I/005/12/0. E. Jiménez-Bailón acknowledges
352 funding by CONACyT research grant 129204 (Mexico). V. Chavushyan acknowledges funding by
353 CONACyT research grant 151494 (Mexico). TOPCAT¹ ([Taylor 2005](#)) has been used in this work
354 for the preparation and manipulation of the tabular data and the images. The WENSS project
355 was a collaboration between the Netherlands Foundation for Research in Astronomy and the
356 Leiden Observatory. We acknowledge the WENSS team consisted of Ger de Bruyn, Yuan Tang,
357 Roeland Rengelink, George Miley, Huub Rottgering, Malcolm Bremer, Martin Bremer, Wim
358 Brouw, Ernst Raimond and David Fullagar for the extensive work aimed at producing the WENSS
359 catalog. Part of this work is based on archival data, software or on-line services provided by the
360 ASI Science Data Center. This research has made use of data obtained from the High Energy
361 Astrophysics Science Archive Research Center (HEASARC) provided by NASA’s Goddard Space
362 Flight Center; the SIMBAD database operated at CDS, Strasbourg, France; the NASA/IPAC
363 Extragalactic Database (NED) operated by the Jet Propulsion Laboratory, California Institute
364 of Technology, under contract with the National Aeronautics and Space Administration. This

¹<http://www.star.bris.ac.uk/~mb t/topcat/>

365 research has made use of software provided by the Chandra X-ray Center (CXC) in the application
366 packages CIAO, ChIPS, and Sherpa. Part of this work is based on the NVSS (NRAO VLA Sky
367 Survey); The National Radio Astronomy Observatory is operated by Associated Universities, Inc.,
368 under contract with the National Science Foundation. This publication makes use of data products
369 from the Two Micron All Sky Survey, which is a joint project of the University of Massachusetts
370 and the Infrared Processing and Analysis Center/California Institute of Technology, funded
371 by the National Aeronautics and Space Administration and the National Science Foundation.
372 This publication makes use of data products from the Wide-field Infrared Survey Explorer,
373 which is a joint project of the University of California, Los Angeles, and the Jet Propulsion
374 Laboratory/California Institute of Technology, funded by the National Aeronautics and Space
375 Administration. Funding for the SDSS and SDSS-II has been provided by the Alfred P. Sloan
376 Foundation, the Participating Institutions, the National Science Foundation, the U.S. Department
377 of Energy, the National Aeronautics and Space Administration, the Japanese Monbukagakusho,
378 the Max Planck Society, and the Higher Education Funding Council for England. The SDSS Web
379 Site is <http://www.sdss.org/>. The SDSS is managed by the Astrophysical Research Consortium for
380 the Participating Institutions. The Participating Institutions are the American Museum of Natural
381 History, Astrophysical Institute Potsdam, University of Basel, University of Cambridge, Case
382 Western Reserve University, University of Chicago, Drexel University, Fermilab, the Institute for
383 Advanced Study, the Japan Participation Group, Johns Hopkins University, the Joint Institute for
384 Nuclear Astrophysics, the Kavli Institute for Particle Astrophysics and Cosmology, the Korean
385 Scientist Group, the Chinese Academy of Sciences (LAMOST), Los Alamos National Laboratory,
386 the Max-Planck-Institute for Astronomy (MPIA), the Max-Planck-Institute for Astrophysics
387 (MPA), New Mexico State University, Ohio State University, University of Pittsburgh, University
388 of Portsmouth, Princeton University, the United States Naval Observatory, and the University of
389 Washington. The United Kingdom Infrared Telescope is operated by the Joint Astronomy Centre
390 on behalf of the Science and Technology Facilities Council of the U.K.

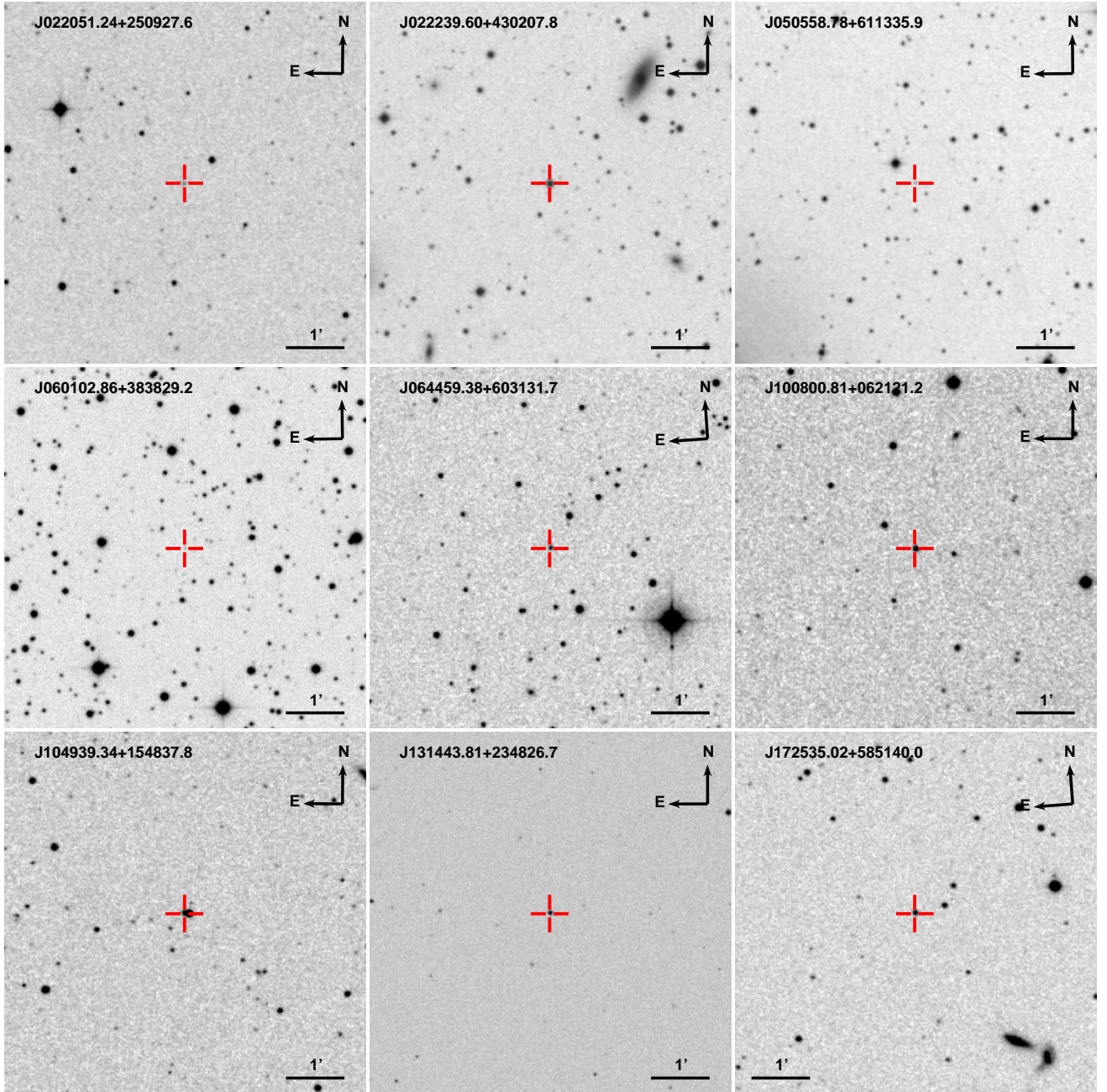


Fig. 1.— Optical images of the fields of 9 of the WISE sources selected in this paper for optical spectroscopic follow-up (see Table 1). The object name, image scale and orientation are indicated in each panel. The proposed optical counterparts are indicated with red marks and the fields are extracted from the DSS-II-Red survey.

Table 2: Main observation properties of WISE sources discussed in this paper. For each source we indicate the name (WISE NAME), the date of the observation (OBS. DATE), the telescope used for the observations (TELESCOPE), the exposure time (EXPOSURE), the rest frame EW of the identified lines (EW), and the estimated redshift (REDSHIFT).

WISE NAME	OBS. DATE	TELESCOPE	EXPOSURE (min)	EW (Å)										REDSHIFT
				Mg II	[Ne V]	[O II]	[Ne III]	Ca II H	Ca II K	H δ	H β	[O III]		
J022051.24+250927.6	2013-01-17	MMT	2×30	30.8 ± 0.7	1.8 ± 0.3	1.7 ± 0.3	1.1 ± 0.4	-	-	-	-	15.8 ± 0.3	0.4818 ± 0.0002	
J050558.78+611335.9	2013-01-18	MMT	2×30	-	-	-	-	-	-	-	-	-	-	
J060102.86+383829.2	2013-01-18	MMT	2×45	-	-	-	-	-	-	-	-	-	-	
J064459.38+603131.7	2013-01-18	MMT	2×30	6.1 ± 0.4	-	-	-	-	-	7 ± 2	4 ± 2	-	0.3582 ± 0.0008	
J104939.34+154837.8	2013-05-02	OAN	3×30	-	-	-	-	0.7 ± 0.1	0.6 ± 0.1	-	-	-	0.3271 ± 0.0003	
J022239.60+430207.8	2012-12-03	Loiano	2×30	-	-	-	-	-	-	-	-	-	-	
J100800.81+062121.2	2013-01-17	MMT	2×30	-	-	-	-	-	-	-	-	-	0.6495*	
J131443.81+234826.7	2013-01-17	MMT	2×30	-	-	-	-	-	-	-	-	-	-	
J172535.02+585140.0	2013-01-17	MMT	2×30	-	-	-	-	-	-	-	-	-	-	

Notes:

* Tentative estimate.

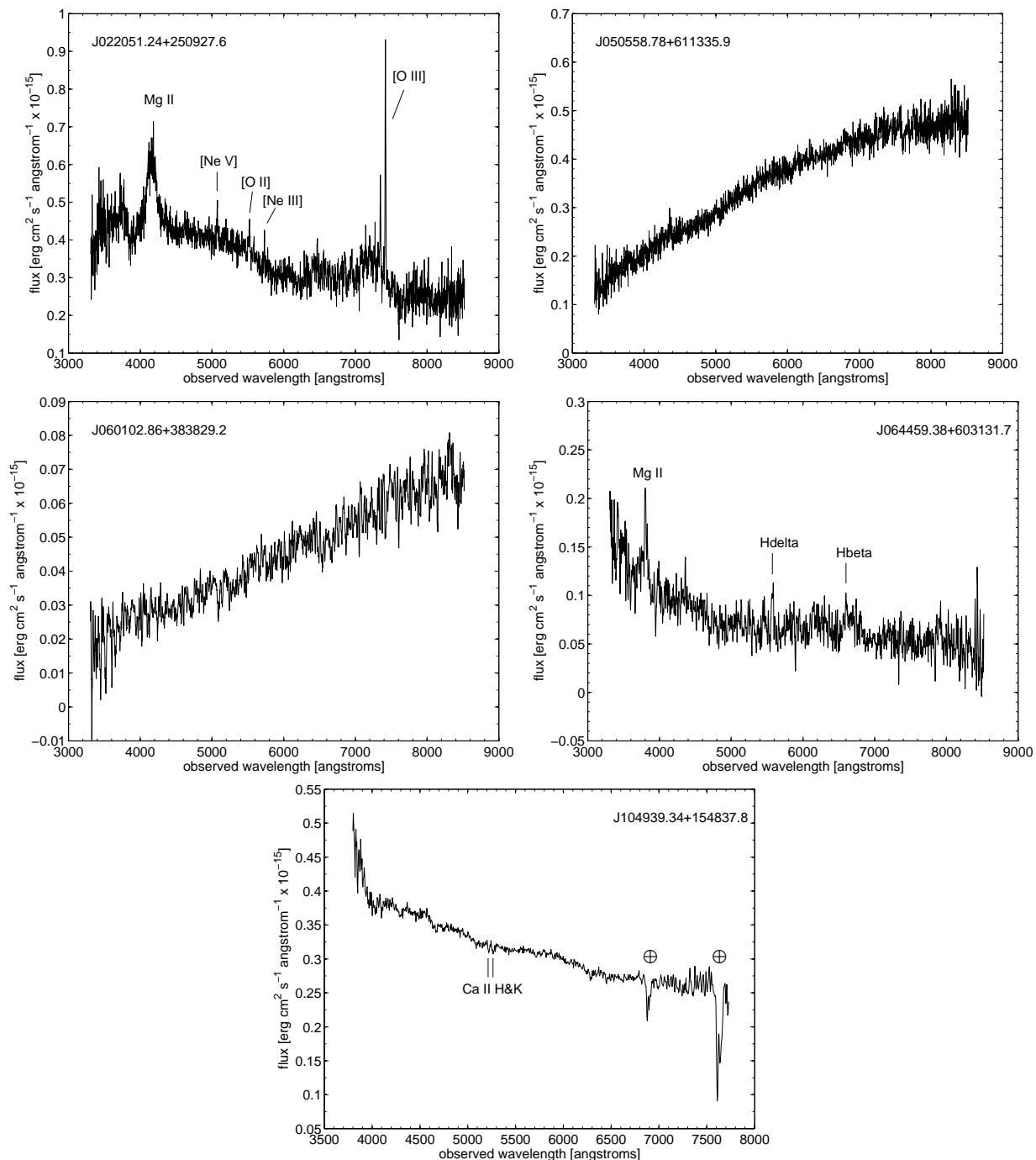


Fig. 2.— Optical spectra obtained with MMT Blue Channel Spectrograph of the four WISE γ -ray blazar candidates associated with *Fermi*-LAT UGS or AGU. The WISE name of each source is indicated in the relative panel, as well as the identified emission lines. With the exception of J104939.34+154837.8, whose spectrum has been obtained with OAN telescope, all other spectra have been obtained with MMT Blue Channel Spectrograph.

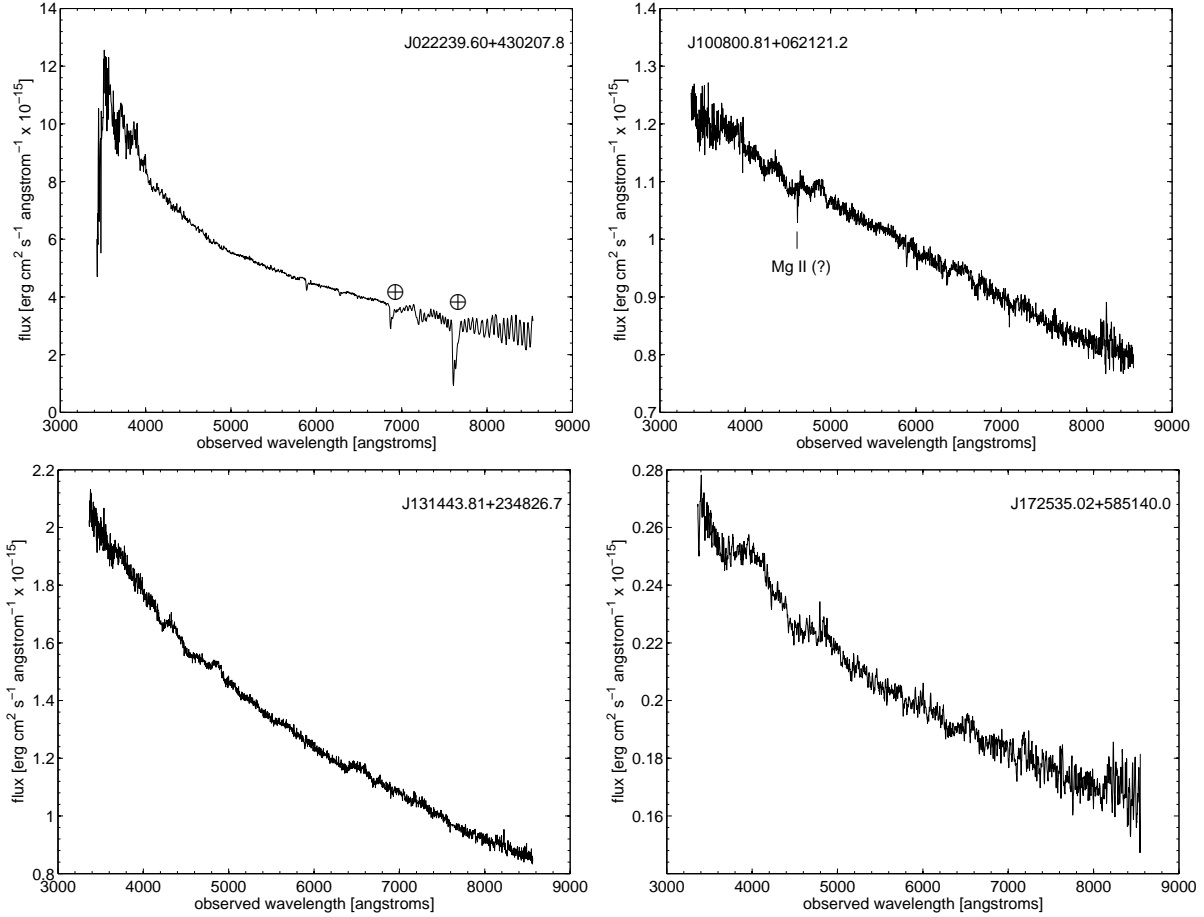


Fig. 3.— Optical spectra of the five WISE sources associated by [D’Abrusco et al. \(2013\)](#) with known *Fermi*-LAT γ -ray blazars. As in Fig. 2, the WISE name of each source is indicated in the relative panel, as well as the identified emission lines. With the exception of J022239.60+430207.8, whose spectrum has been obtained with Loiano telescope, all other spectra have been obtained with MMT Blue Channel Spectrograph.

REFERENCES

391

392 Abdo A. A., et al., 2013, in preparation

393 Ackermann M., et al., 2011, ApJ, 743, 171

394 Aharonian F., et al., 2009, A&A, 502, 749

395 Arnaud K. A., 1996, ASPC, 101, 17

396 Becker R. H., White R. L., Helfand D. J., 1995, ApJ, 450, 559

397 Blandford R. D., Rees M. J., 1978, Proc. “Pittsburgh Conference on BL Lac objects”, 328

398 Bourda G., Collioud A., Charlot P., Porcas R., Garrington S., 2011, A&A, 526, A102

399 Butcher H. R., Oemler A., Jr., Tapia S., Tarenghi M., 1976, ApJ, 209, L11

400 Capalbi M., Perri M. Saija B. Tamburelli F., Angelini L. 2005,

401 http://heasarc.nasa.gov/docs/swift/analysis/xrt_swguide_v1_2.pdf

402 Cardelli J. A., Clayton G. C., Mathis J. S., 1989, ApJ, 345, 245

403 Condon J. J., Cotton W. D., Greisen E. W., Yin Q. F., Perley R. A., Taylor G. B., Broderick J. J.,

404 1998, AJ, 115, 1693

405 Cowperthwaite P. S., Massaro F., D’Abrusco R., Paggi A., Tosti G., Smith H. A., 2013, arXiv,

406 arXiv:1308.1950

407 D’Abrusco R., Longo G., Walton N. A., 2009, MNRAS, 396, 223

408 D’Abrusco R., Massaro F., Ajello M., Grindlay J. E., Smith H. A., Tosti G., 2012, ApJ, 748, 68

409 D’Abrusco R., Massaro F., Paggi A., Masetti N., Tosti G., Giroletti M., Smith H. A., 2013, ApJS,

410 206, 12

- ⁴¹¹ D’Elia V., et al., 2013, *A&A*, 551, A142
- ⁴¹² Dermer C. D., Schlickeiser R., 1993, *ApJ*, 416, 458
- ⁴¹³ Dermer C. D., Finke J. D., Krug H., Böttcher M., 2009, *ApJ*, 692, 32
- ⁴¹⁴ Fermi collaboration, 2013, *ApJ*, in preparation
- ⁴¹⁵ Finke J. D., Shields J. C., Böttcher M., Basu S., 2008, *A&A*, 477, 513
- ⁴¹⁶ Freeman P., Doe S., Siemiginowska A., 2001, *SPIE*, 4477, 76
- ⁴¹⁷ Fruscione A., et al., 2006, *SPIE*, 6270
- ⁴¹⁸ Furniss A., Fumagalli M., Danforth C., Williams D. A., Prochaska J. X., 2013, *ApJ*, 766, 35
- ⁴¹⁹ Giommi P., Padovani P., Polenta G., Turriziani S., D’Elia V., Piranomonte S., 2012, *MNRAS*, 420,
⁴²⁰ 2899
- ⁴²¹ Giommi P., Padovani P., Polenta G., 2013, *MNRAS*, 431, 1914
- ⁴²² Inoue S., Takahara F., 1996, *ApJ*, 463, 555
- ⁴²³ Kalberla P. M. W., Burton W. B., Hartmann D., Arnal E. M., Bajaja E., Morras R., Pöppel
⁴²⁴ W. G. L., 2005, *A&A*, 440, 775
- ⁴²⁵ Kinney A. L., Bohlin R. C., Blades J. C., York D. G., 1991, *ApJS*, 75, 645
- ⁴²⁶ Landt H., Bignall H. E., 2008, *MNRAS*, 391, 967
- ⁴²⁷ Laurent-Muehleisen S. A., Kollgaard R. I., Feigelson E. D., Brinkmann W., Siebert J., 1999, *ApJ*,
⁴²⁸ 525, 127
- ⁴²⁹ Laurino O., D’Abrusco R., Longo G., Riccio G., 2011, *MNRAS*, 418, 2165
- ⁴³⁰ Linford J. D., et al., 2011, *ApJ*, 726, 16

- 431 Linford J. D., Taylor G. B., Romani R. W., Helmboldt J. F., Readhead A. C. S., Reeves R.,
432 Richards J. L., 2012, ApJ, 744, 177
- 433 Londish D., Heidt J., Boyle B. J., Croom S. M., Kedziora-Chudczer L., 2004, MNRAS, 352, 903
- 434 Mao L. S., 2011, NewA, 16, 503
- 435 Marleau F. R., Fadda D., Appleton P. N., Noriega-Crespo A., Im M., Clancy D., 2007, ApJ, 663,
436 218
- 437 Massaro E., Giommi P., Leto C., Marchegiani P., Maselli A., Perri M., Piranomonte S., 2011a,
438 bzc3.book
- 439 Massaro F., D’Abrusco R., Ajello M., Grindlay J. E., Smith H. A., 2011b, ApJ, 740, L48
- 440 Massaro F., D’Abrusco R., Tosti G., Ajello M., Gasparrini D., Grindlay J. E., Smith H. A., 2012a,
441 ApJ, 750, 138
- 442 Massaro F., D’Abrusco R., Paggi A., Masetti N., Giroletti M., Tosti G., Smith H. A., Funk S.,
443 2013a, ApJS, 206, 13
- 444 Massaro F., D’Abrusco R., Giroletti M., Paggi A., Masetti N., Tosti G., Nori M., Funk S., 2013b,
445 ApJS, 207, 4
- 446 Massaro F., et al., 2013c, ApJS in press
- 447 Matheson, T., et al., 2008, AJ, 135, 1598
- 448 Miller J. S., French H. B., Hawley S. A., 1978, bllo.conf, 176
- 449 Monet D. G., et al., 2003, AJ, 125, 984
- 450 Moretti A., et al., 2005, SPIE, 5898, 360
- 451 Nolan P. L., et al., 2012, ApJS, 199, 31

- ⁴⁵² Paggi A., et al., 2013, ApJS, in press
- ⁴⁵³ Pâris I., et al., 2012, A&A, 548, A66
- ⁴⁵⁴ Perri M., et al., 2007, A&A, 462, 889
- ⁴⁵⁵ Petrov L., 2011, AJ, 142, 105
- ⁴⁵⁶ Prandini E., Bonnoli G., Maraschi L., Mariotti M., Tavecchio F., 2010, MNRAS, 405, L76
- ⁴⁵⁷ Puccetti S., et al., 2011, A&A, 528, A122
- ⁴⁵⁸ Rengelink R. B., Tang Y., de Bruyn A. G., Miley G. K., Bremer M. N., Roettgering H. J. A.,
⁴⁵⁹ Bremer M. A. R., 1997, A&AS, 124, 259
- ⁴⁶⁰ Richards G. T., et al., 2004, ApJS, 155, 257
- ⁴⁶¹ Shaw M. S., et al., 2013, ApJ, 764, 135
- ⁴⁶² Shemmer O., et al., 2006, ApJ, 644, 86
- ⁴⁶³ Shemmer O., Brandt W. N., Anderson S. F., Diamond-Stanic A. M., Fan X., Richards G. T.,
⁴⁶⁴ Schneider D. P., Strauss M. A., 2009, ApJ, 696, 580
- ⁴⁶⁵ Skrutskie M. F., et al., 2006, AJ, 131, 1163
- ⁴⁶⁶ Stickel M., Padovani P., Urry C. M., Fried J. W., Kuehr H., 1991, ApJ, 374, 431
- ⁴⁶⁷ Stocke J. T., Rector T. A., 1997, ApJ, 489, L17
- ⁴⁶⁸ Taylor M. B., 2005, ASPC, 347, 29
- ⁴⁶⁹ Urrutia T., Becker R. H., White R. L., Glikman E., Lacy M., Hodge J., Gregg M. D., 2009, ApJ,
⁴⁷⁰ 698, 1095
- ⁴⁷¹ Urry C. M., Padovani P., 1995, PASP, 107, 803

⁴⁷² Wright E. L., et al., 2010, AJ, 140, 1868

⁴⁷³ Wurtz R., Ellingson E., Stocke J. T., Yee H. K. C., 1993, AJ, 106, 869

⁴⁷⁴ Wurtz R., Stocke J. T., Ellingson E., Yee H. K. C., 1997, ApJ, 480, 547

⁴⁷⁵ Yang J., Wang J., 2010, PASJ, 62, L23

476

A. SEDs

477 SEDs of the sources listed in Table 1 are presented in Figures 4 and 5. For each source we
478 show the spectral points corresponding to the various counterparts we found in a standard 3.3''
479 searching radius (see D'Abrusco et al. 2013). Circles represent detections, while down triangles
480 represent upper limits, with the color code presented in the legends. For IR, optical and UV
481 points we present de-reddened fluxes obtained using the extinction law presented by Cardelli,
482 Clayton, & Mathis (1989) and the galactic extinction value as derived by the Infrared Science
483 Archive² (IRSA). The XRT data were processed using the XRTDAS software (Capalbi et al.
484 2005) developed at the ASI Science Data Center and included in the HEASoft package (v. 6.13)
485 distributed by HEASARC. For each observation of the sample, calibrated and cleaned PC mode
486 event files were produced with the XRTPIPELINE task (ver. 0.12.6), producing exposure maps for
487 each observation. In addition to the screening criteria used by the standard pipeline processing,
488 we applied a further filter to screen background spikes that can occur when the angle between
489 the pointing direction of the satellite and the bright Earth limb is low. In order to eliminate this
490 so called bright Earth effect, due to the scattered optical light that usually occurs towards the
491 beginning or the end of each orbit, we used the procedure proposed by Puccetti et al. (2011) and
492 D'Elia et al. (2013). We monitored the count rate on the CCD border and, through the XSELECT
493 package, we excluded time intervals when the count rate in this region exceeded 40 counts/s;
494 moreover, we selected only time intervals with CCD temperatures less than -50°C (instead of
495 the standard limit of -47°C) since contamination by dark current and hot pixels, which increase
496 the low energy background, is strongly temperature dependent (D'Elia et al. 2013). We then
497 proceeded to merge cleaned event files obtained with this procedure using XSELECT, considering
498 only observations with telescope aim point falling in a circular region of 10' radius centered in
499 the median of the individual aim points, in order to have a uniform exposure. The corresponding

²<http://irsa.ipac.caltech.edu/applications/DUST/>

500 merged exposure maps were then generated by summing the exposure maps of the individual
501 observations with `XIMAGE` (ver. 4.5.1). When possible, *Swift* XRT-PC spectra are obtained from
502 merged events extracted with `XRTPRODUCTS` task using a 20 pixel radius circle centered on the
503 coordinates reported in Table 1 and background estimated from a nearby source-free circular
504 region of 20 pixel radius. When the source count rate is above $0.5 \text{ counts s}^{-1}$, the data are
505 significantly affected by pileup in the inner part of the point-spread function (Moretti et al. 2005).
506 To remove the pile-up contamination, we extract only events contained in an annular region
507 centered on the source (e.g., Perri et al. 2007). The inner radius of the region was determined
508 by comparing the observed profiles with the analytical model derived by Moretti et al. (2005)
509 and typically has a 4 or 5 pixels radius, while the outer radius is 20 pixels for each observation.
510 Source spectra are binned to ensure a minimum of 20 counts per bin in order to ensure the
511 validity of χ^2 statistics. We performed our spectral analysis with the `SHERPA`³ modeling and fitting
512 application (Freeman, Doe, & Siemiginowska 2001) include in the CIAO (Fruscione et al. 2006)
513 4.5 software package, and with the `XSPEC` software package, version 12.8.0 (Arnaud 1996) with
514 identical results. For the spectral fitting we used a model comprising an absorption component
515 fixed to the Galactic value (Kalberla et al. 2005) and a powerlaw, and we plot intrinsic fluxes (i.e.,
516 without Galactic photoelectric absorption). When the extracted counts are not enough to provide
517 acceptable spectral fits we simply converted the extracted count rates to 0.3-10 keV intrinsic
518 fluxes with `PIMMS`⁴ 4.6b software, assuming a powerlaw spectra with spectral index 2 and an
519 absorption component fixed to the Galactic value, and in this case we report with a filled circle the
520 flux corresponding to the extracted countrate.

³<http://cxc.harvard.edu/sherpa>

⁴<http://heasarc.nasa.gov/docs/journal/pimms3.html>

Fig. 4.— SEDs of γ -ray blazar candidates listed in the upper part of Table 1. Symbol description is given in Appendix A.

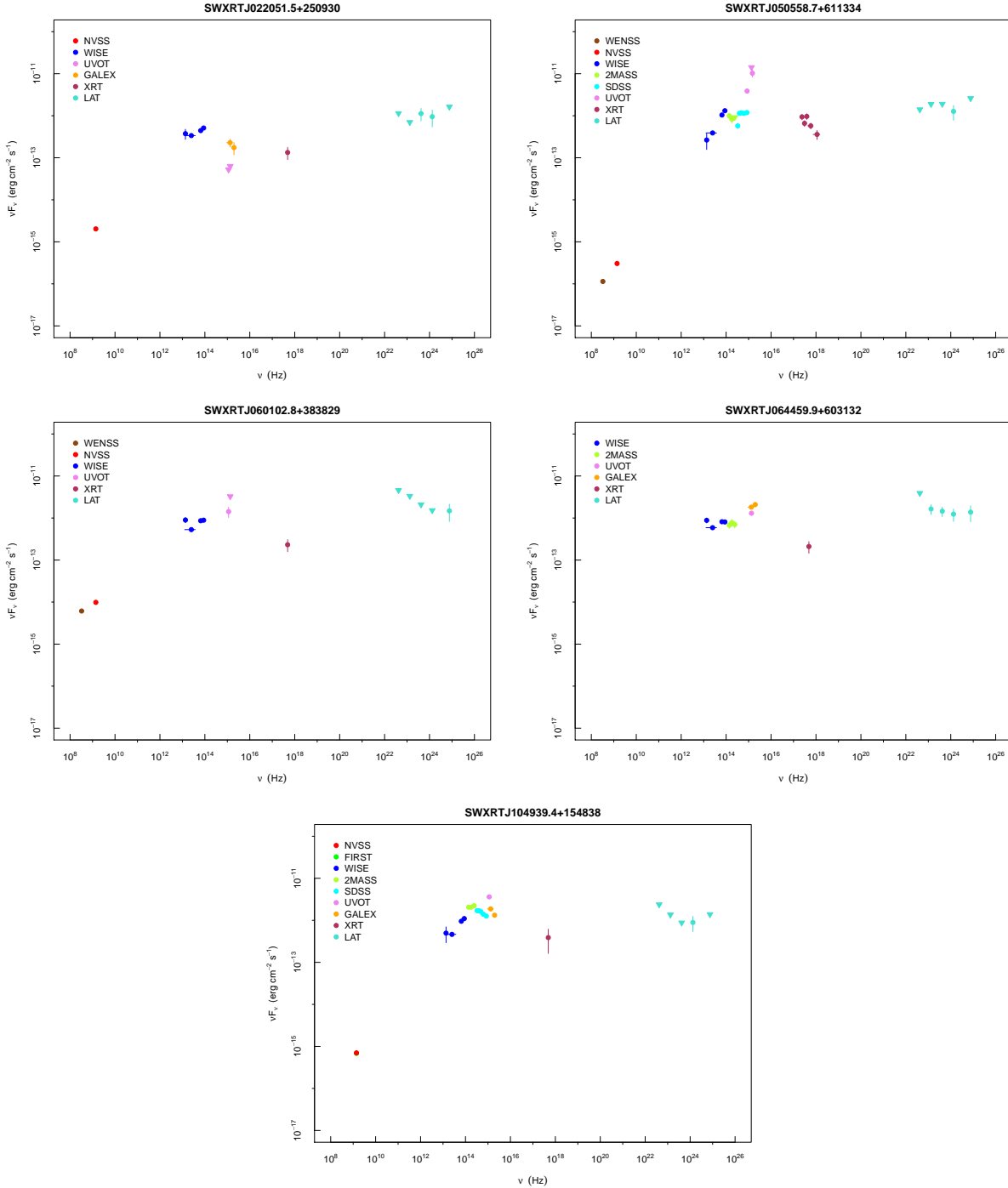


Fig. 5.— SEDs of γ -ray blazar candidates listed in the lower part of Table 1. Symbol description is given in Appendix A.

